Calhoun: The NPS Institutional Archive

Theses and Dissertations Thesis Collection

1994-09

An analysis of orbital propagators for low earth orbit rendezvous

Pollock, Kenneth R.

Monterey, California. Naval Postgraduate School

---

http://hdl.handle.net/10945/43012

Calhoun is a project of the Dudley Knox Library at NPS, furthering the precepts and goals of open government and government transparency. All information contained herein has been approved for release by the NPS Public Affairs Officer.

Dudley Knox Library / Naval Postgraduate School
411 Dyer Road / 1 University Circle
Monterey, California USA 93943

http://www.nps.edu/library

NAVAL POSTGRADUATE SCHOOL
MONTEREY, CALIFORNIA

DTIC
ELECTE
DEC 19 1994
G

THESIS

AN ANALYSIS OF ORBITAL PROPAGATORS FOR LOW EARTH ORBIT RENDEZVOUS

by

Kenneth R. Pollock

September 1994

Thesis Advisor: Clyde Scandrett

Approved for public release; distribution is unlimited

DTIC QUALITY INSPECTED 1

19941214 017

REPORT DOCUMENTATION PAGE

Form Approved
OMB No. 0704-0188

Public reporting burden for this collection of information is estimated to average 1 hour per response, including the time for reviewing instructions, searching existing data sources, gathering and maintaining the data needed, and completing and reviewing the collection of information. Send comments regarding this burden estimate or any other aspect of this collection of information, including suggestions for reducing this burden, to Washington Headquarters Services, Directorate for information Operations and Reports, 1215 Jefferson Davis Highway, Suite 1204, Arlington, VA 22202-4302, and to the Office of Management and Budget, Paperwork Reduction Project (0704-0188), Washington, DC 20503.

1. AGENCY USE ONLY *(leave Blank)*	2. REPORT DATE September 1994	3. REPORT TYPE AND DATES COVERED Master's Thesis

4. TITLE AND SUBTITLE
AN ANALYSIS OF ORBITAL PROPAGATORS FOR LOW EARTH ORBIT RENDEZVOUS

5. FUNDING NUMBERS

6. AUTHOR(S)
Pollock, Kenneth R.

7. PERFORMING ORGANIZATION NAME(S) AND ADDRESS(ES)
Naval Postgraduate School
Monterey, CA 93943-5000

8. PERFORMING ORGANIZATION REPORT NUMBER

9. SPONSORING/MONITORING AGENCY NAME(S) AND ADDRESS(ES)

10. SPONSORING/MONITORING AGENCY REPORT NUMBER

11. SUPPLEMENTARY NOTES
The views expressed in this thesis are those of the author and do not reflect the official policy or positions of the Department of Defense or the U.S. Government.

12a. DISTRIBUTION/AVAILABILITY STATEMENT
Approved for public release; distribution is unlimited.

12b. DISTRIBUTION CODE

13. ABSTRACT *(Maximum 200 words)*

This thesis examines the performance of three different orbital propagators to determine which provide the best performance for use in Low Earth Orbit Rendezvous. The performance evaluation is based upon the propagator's accuracy and the amount of time required to produce a solution. A Cowell high-fidelity propagator is used as a base line for comparison with an Encke and Clohessy-Wiltshire propagator. To further enhance the examination a Jacchia-70 atmospheric model and a GEM-9 Geopotential model are used to provide perturbing acceleration inputs to the propagators. All comparisons are performed in a Local Vertical, Local Horizontal Reference Frame with the target spacecraft at the coordinate center. Tainting of the input data set by a prior processor make the findings suspect. Findings support the prediction that while the Cowell propagator is the most accurate it also takes the most time to achieve results. Also, the Clohessy-Wiltshire, while taking the least time is the most inaccurate. The Encke propagator deliveries the most balanced result.

14.SUBJECT TERMS
Orbital, Rendezvous, Propagator

15. NUMBER OF PAGES
61

16. PRICE CODE

17. SECURITY CLASSIFICATION OF REPORT Unclassified	18. SECURITY CLASSIFICATION OF THIS PAGE Unclassified	19. SECURITY CLASSIFICATION OF ABSTRACT Unclassified	20. LIMITATION OF ABSTRACT UL

NSN 7540-01-280-5500

Standard Form 298 (Rev. 2-89)
Prescribed by ANSI Std. Z39-18

Approved for public release; distribution is unlimited

AN ANALYSIS OF ORBITAL PROPAGATORS FOR LOW EARTH ORBIT RENDEZVOUS

Kenneth R. Pollock
Lieutenant, United States Navy
B.A., University of Virginia, 1988

Submitted in partial fulfillment of the
requirements for the degree of

MASTER OF SCIENCE IN ASTRONAUTICAL ENGINEERING

from the

NAVAL POSTGRADUATE SCHOOL
September 1994

Accesion For
NTIS CRA&I ☒
DTIC TAB ☐
Unannounced ☐
Justification
By
Distribution /
Availability Codes
Dist | Avail and / or Special
A-1

Author: [redacted]
Kenneth R. Pollock

Approved by: [redacted]
[redacted]sis Advisor

[redacted]
I. Michael Ross, Second Reader

[redacted]
Daniel J. Collins, Chairman
Department of Aeronautics and Astronautics

ABSTRACT

This thesis examines the performance of three different orbital propagators to determine which provide the best performance for use in Low Earth Orbit Rendezvous. The performance evaluation is based upon the propagator's accuracy and the amount of time required to produce a solution. A Cowell high-fidelity propagator is used as a base line for comparison with an Encke and Clohessy-Wiltshire propagator. To further enhance the examination a Jacchia-70 atmospheric model and a GEM-9 Geopotential model are used to provide perturbing acceleration inputs to the propagators. All comparisons are performed in a Local Vertical, Local Horizontal Reference Frame with the target spacecraft at the coordinate center. Tainting of the input data set by a prior processor make the findings suspect. Findings support the prediction that while the Cowell propagator is the most accurate it also takes the most time to achieve results. Also, the Clohessy-Wiltshire, while taking the least time is the most inaccurate. The Encke propagator deliveries the most balanced result.

TABLE OF CONTENTS

I INTRODUCTION 1

II. REFERENCE FRAMES 5

- A. THE M-50 INERTIAL REFERENCE FRAME 6
- B. WGS-84 EARTH CENTERED EARTH FIXED REFERENCE FRAME 6
- C. RELATIVE MOTION REFERENCE FRAME 7
  - 1. Local Vertical, Local Horizontal Coordinate System 7
  - 2. Roll, Pitch and Yaw Coordinate System 8
- D. COORDINATE TRANSFORMATION 9

III. THE PROPAGATORS 11

- A. THE COWELL PROPAGATOR 12
- B. THE CLOHESSY-WILTSHIRE PROPAGATOR 13
- C. THE ENCKE PROPAGATOR 17

IV. THE PERTURBING ACCELERATIONS 21

- A. THE PERTURBATIONS 21
  - 1. Solar Pressure 21
  - 2. Magnetic 22
  - 3. Third Body Effects 22
  - 4. Earth Gravity Harmonics 23
  - 5. Atmospheric Drag 24
- B. THE MODELS 25
  - 1. The GEM-9 Geopotential Model 25
  - 2. The Jacchia 71 Atmospheric Model 25

V. COMPARING PROPAGATORS 27

- A. THE DATA SET 27
- B. THE PROGRAMS 28
- C. PERFORMANCE 29
- D. FINDINGS 30
- E. COMPUTATION TIME 38

VI. CONCLUSIONS 43

- A. RESULTS 43
- B. ADDITIONAL WORK 44
  - 1. Raw Data 44
  - 2. Encke Propagator 44
  - 3. Repeated Iterations 44
  - 4. Different Orbits 45

LIST OF REFERENCES 47

INITIAL DISTRIBUTION LIST 49

ACKNOWLEDGMENT

This thesis is a follow-up to work performed by a pair of Naval Officers during their time at the Naval Postgraduate School. LT Lester Makepeace and LT Lee Barker performed much of the preliminary work in the theory and computer programming which created the orbit propagators used in this thesis. In fact, it was “Les’ Law” , that two satellites in nearly the same orbit are perturbed identically, which provided the initial motivation behind this thesis.

I would like to thank Jack Brazzel and Scott Tamblyn for providing assistance in developing both the thesis concept and the Clohessy-Wiltshire propagator. I would also like to thank the Astronaut Office at the Johnson Space Center for their cooperation and support in my initial research. Additional acknowledgment must go to Dr David Carter of Draper Labs for his aid in developing the Jacchia-70 atmospheric model.

Lastly, I must thank my wife Heidi for her patience and understanding. Despite having to plan a wedding at the same time, she continued to support me and keep me going. Without her I could never have done this.

I. INTRODUCTION

The intercept of two large objects in a gravity free environment can either be very easy or very hard depending on whether or not you want both objects intact after the meeting. If not, a high energy collision works every time. For rendezvous in space, the object is for two spacecraft to meet in space, work together and separate with no damage to either. This requires a great deal of knowledge and planning involving a medium in which human beings have little intuition. To counter this shortcoming tools have developed to help.

Orbital propagators have been used for years to predict the positions and velocities of objects in orbit. They are an integral part of space navigation. Their only real shortcoming is their size and complexity. A good high fidelity propagator can involve thousands of lines of code and many minutes of processing time in order to predict a spacecraft's orbital location. While this is acceptable for mission planning, it is not very useful for real-time propagation.

In September of 1993 NASA launched STS-51 which experimented with a new navigational tool. The Detailed Technical Objective 700, consisted of a GRID laptop computer with software written by NASA and a group of students from the Naval Postgraduate School (Ref. 1). As a precursor to an automated navigational system, this experiment was designed to demonstrate how on-orbit orbital prediction and graphical displays could assist astronauts navigating of the Shuttle Orbiter. Such an aid was found to be especially valuable during Proximity Operations and Rendezvous (Ref. 1). The programs RPOP and NPSLite flew and were used during an actual rendezvous.

The problem with RPOP or NPSLite as bases for an automated navigation program lays in their design. RPOP used a set of differential equations developed by Clohessy-Wiltshire for orbital prediction while NPSLite used a "f" and "g" function type propagator (Ref. 1). Neither of the propagators took into account perturbations caused by external forces except those inherent in the Two Body Problem. This was not an arbitrary decision. Normally the equations used to determine orbital position for a two body problem are not that complex, and therefore fairly simple for a computer to handle. The addition of various gravitation and atmospheric models to more accurately reflect small perturbing accelerations can greatly increase both program size and processing time. In the case of RPOP and NPSLite, it was assumed that two objects in nearly identical orbits are perturbed relatively the same. Therefore, when dealing with a purely relative reference frame these perturbations could be ignored with little loss of accuracy. The purpose of this thesis is to determine the validity of that assumption.

As a result of the success of RPOP and NPSLite, NASA has decided to develop a flight qualified version of the RPOP software. It is NASA's intention to have the software available for use during the future Space Shuttle - MIR mission in 1995. One of the difficulties in the flight certification is verifying that the algorithm upon which the software is based is sufficiently accurate. By expanding this query, we can quickly find ourselves asking which of the many orbital propagation models and algorithms available is the best for the purpose at hand. This is the second objective of this thesis.

As previously mentioned, the on-orbit computation time a propagator requires can be critical. In order to be useful for the flight crew, a propagator should accurately predict the Orbiter's position and velocity at least one orbit, approximately 90 minutes, in advance. Because even the most accurate propagator is vulnerable to errors, this 90 minute requirement must be broken up into a series of steps typically on the order of a few seconds. This in turn means that the propagator must provide thousands of predictions for each 90 minute propagation. Additionally, to be of any use on-orbit, the software needs to perform all of these predictions repeatably every few seconds. For a high fidelity, time intensive propagator, this time restriction may render the algorithm of little value.

Because of the time constraint, the best propagator is not necessarily the most useful. The best propagator balances accuracy with low computation time. An ideal propagator would be best in both categories, but as will be seen this is rarely if ever the case. In fact, the ideal propagator may eventually depend on far more than just accuracy and speed, but for the moment this study will be limited to just these two criteria. It is the intent of this thesis to provide the initial look and possibly a guideline to future research in the ultimate choice of a best orbit propagation model and algorithm.

II. REFERENCE FRAMES

Which reference frame a body is being observed in is integral to defining and describing the forces interacting with it. By definition, the Newton's laws of motion apply only in an inertial reference frame. In order to translate to a non-inertial reference frame and use the same laws, one must translate those laws into an appropriate form.

Integral to the definition of a reference frame is the coordinate system used to define location within said frame. Basically, all a coordinate system does is determine the location of a point in space relative to another arbitrary point. While this may sound simple, it is extremely important because it allows for the comparison of two objects within the same reference frame. This comparison and the forces which act between and on the objects is normally the true goal of the investigation.

Typically a reference frame and coordinate system are chosen in such a way as to simplify the problem. An example which is directly applicable to this thesis is the relative reference frame. In comparing two objects which are both in motion relative to an inertial reference frame it greatly simplifies the problem if a reference frame and coordinate system is fixed to one object.

For this thesis three different reference frames/coordinate systems are applicable. Primarily among these is the inertial reference frame in which all physical laws are based. Since the two objects of interest are both orbiting the Earth it is natural to remove the rotation of the Earth about its axis as a simplification. This involves an Earth Centered Earth Fixed (ECEF) reference frame/coordinate system. The relative reference frame uses one of the spacecraft as the center of the frame in order to eliminate any identical orbital motion between the two crafts. In all three cases transformation have been developed in order to translate between any of the coordinate systems without loss of accuracy.

A. THE M-50 INERTIAL REFERENCE FRAME

Inertial by definition is a reference frame which is fixed in space or is moving with a constant velocity. The Inertial Reference Frame used by this thesis was the NASA standard M-50 frame. The choice of this frame was obvious because the data supplied by NASA for this thesis was given in terms of these coordinates. It is displayed in Figure 2.1, as a three dimensional, rectilinear system defined by x, y and z axes. The x axis is defined by the Earth's Vernal Equinox or the First Point of Aries. The z axis coincides with the Earth's rotation vector, and roughly points toward the star Polaris. The y axis is defined by the cross products of the x and z axis unit vectors.

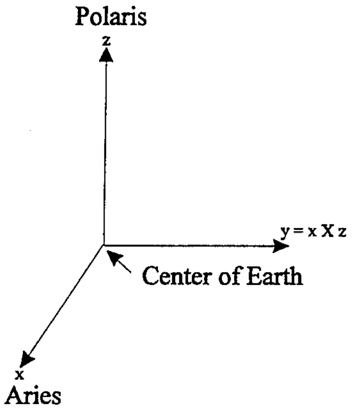

Figure 2.1 Inertial Reference Frame

The M-50 reference frame is Earth centered but the Earth does rotate relative to the frame. Because the Earth also is in motion about the Sun it could be argued that this is not truly an inertial reference frame. While this is true, a Geocentric Inertial Frame is sufficiently accurate for this investigation as long as the speeds involved are not very large relative to the speed of light, because then that Newtonian mechanics must be replaced with Einsteinian.

B. WGS-84 EARTH CENTERED EARTH FIXED REFERENCE FRAME

In order to eliminate unnecessary complications caused by the Earth's rotation an Earth Centered Earth Fixed reference frame is used. The use of this reference frame was also necessitated by the fact that the GEM-9 Gravity Model uses the WGS-84 coordinate system. Again, as seen in Figure 2.2, the WGS-84 is a three dimensional, rectilinear system defined by x, y and z axes. The z axis is defined by the Earth's spin axis while the x axis is in this case defined by 0° Latitude and Longitude. Again the y axis is defined by the cross product of the x and z unit vectors. The entire reference frame is in rotation about the z axis at a rate equal to the Earth's rotation rate.

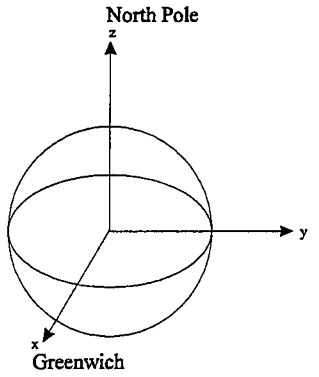

Figure 2.2 Earth Centered, Earth Fixed Coordinate System

C. RELATIVE MOTION REFERENCE FRAME

The relative motion reference frame is where most of the work takes place. Because we are looking at two objects orbiting the Earth in near identical paths, much of the orbital motion can be ignored. It is logical to assume that forces acting on the two objects identically in an inertial or ECEF reference frame can also be ignored with little loss in accuracy when a relative system is adopted. Whether this assumption is true or not is the subject of this thesis.

There are two potential coordinate systems. The first is called Local Vertical, Local Horizontal (LVLH) and is defined relative to the orbit of the spacecraft, while the second is called Roll, Pitch and Yaw (RPY), is defined relative to the spacecraft itself. Both have advantages or disadvantages depending on what is required.

1. Local Vertical, Local Horizontal Coordinate System

LVLH is again a rectilinear system with x, y, and z coordinates. The x axis is defined by the direction of motion while the z axis points radially outward from the Earth.

The y axis is defined by the cross product of the x and z axis. As seen in Figure 2.3 the horizontal plane is defined by the x and y axis and the vertical plane by the x and z axis. A LVLH coordinate system is in constant rotation relative to an ECEF coordinate system (typically about the y axis.) The magnitude of that rotation is equal to the spacecraft's angular velocity about the Earth's center. Since the LVLH coordinate system is based upon the object's orbit and not it's attitude and because the orbiting objects are small relative to the earth, they can normally be treated as point masses.

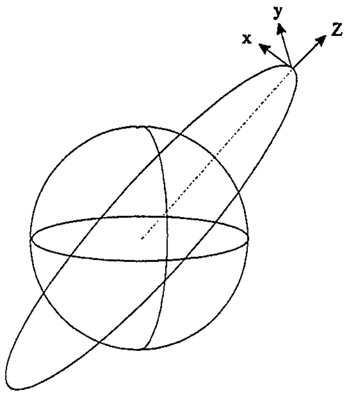

Figure 2.3 Local Vertical, Local Horizontal Coordinate System

2. Roll, Pitch and Yaw Coordinate System

The RPY coordinate system is identical to that of an aircraft's with the x or roll axis pointing out the nose of the spacecraft, the z or yaw axis out the spacecraft's belly and the y or pitch axis pointing out the starboard wing. See Figure 2.4 for a graphical representation of this coordinate system. This is a very advantageous system for any sensors or personnel located on the spacecraft, but since the spacecraft may be in rotation about its center of mass it is not ideal when discussing the motion between two orbiting objects.

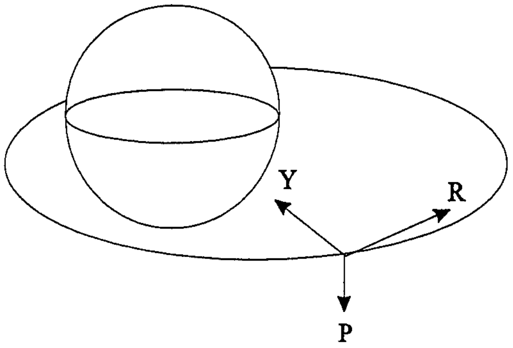

Figure 2.4 Roll, Pitch and Yaw Coordinate System

D. COORDINATE TRANSFORMATIONS

As discussed previously, it is critically important to be able to translate coordinates and forces between the various reference frames in order it insure the accuracy of the Equations of Motion used. The translation process can be a complex one involving detailed math, resulting in the addition of many new forcing terms into the Equations of Motion. These pseudo-forces, while having no existence in inertial space are very important in a rotating reference frame. Fortunately, many of these terms cancel when dealing with relative motion.

The fact that all coordinate systems used are rectilinear is convenient because transformation matrices between systems exist and are well known. Typically a transformation can be view as a series of three rotations about the coordinate axis such that one coordinate system is translated into the other. The rotation about a single axis can be seen in Figure 2.5 .

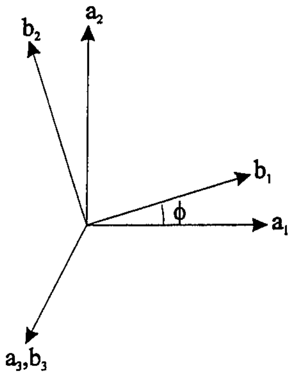

Figure 2.5 Axis Rotation

Mathematically this rotation can be done by multiplying a vector by a rotational matrix to get the rotated coordinates. This rotational matrix is determined from the unit vectors of the two axis.

$$ {}^{A}C^{B} = \begin{bmatrix} \hat{a}_1 \cdot \hat{b}_1 & \hat{a}_1 \cdot \hat{b}_2 & \hat{a}_1 \cdot \hat{b}_3 \\ \hat{a}_2 \cdot \hat{b}_1 & \hat{a}_2 \cdot \hat{b}_2 & \hat{a}_2 \cdot \hat{b}_3 \\ \hat{a}_3 \cdot \hat{b}_1 & \hat{a}_3 \cdot \hat{b}_2 & \hat{a}_3 \cdot \hat{b}_3 \end{bmatrix} = \begin{bmatrix} \cos\phi & \sin\phi & 0 \\ -\sin\phi & \cos\phi & 0 \\ 0 & 0 & 1 \end{bmatrix} \tag{2.1} $$

The rotational matrix in Equation 2.1 can then be multiplied with two other rotational matrices to get the final transformation. The order of the multiplication is important as are the order of the rotations, to insure that the x axis in the first coordinate system lines up with the x axis in the new coordinate system.

$$ {}^{I}C^{E} = \left[{}^{I}C^{A}\right]\left[{}^{A}C^{B}\right]\left[{}^{B}C^{E}\right] \tag{2.2} $$

Transformation matrices were generated and used in translations between all coordinate systems to insure proper accuracy of the data.

III. THE PROPAGATORS

The purpose of any propagator is to accurately predict a spacecraft's position and velocity at some future point in time. There are many different mathematical methods to produce these future vectors, each with their own advantages and shortcomings. While they may differ in application or procedure, all claim Newton's Universal Law of Gravity, Equation 3.1, as their source.

$$F = \frac{Gm_1 m_2}{r^2} \tag{3.1}$$

where G is the Universal Gravitational Constant and r is the distance separating the point masses m_1 and m_2.

To properly apply this physical law to the case of orbital mechanics, some general assumptions must be made. The first is that the two objects of interest are point masses which is valid if we assume the bodies are either spherically symmetrical or relatively small. Secondly, it is assumed that these two point masses are the only ones in the system. In the case of an object orbiting the Earth, the assumption of two point masses gives a sufficiently accurate answer. Given these underlying assumptions and applying Newton's Third Law of Motion we obtain Equation 3.2 which is the equation of the force on an orbiting spacecraft.

$$m\ddot{\bar{r}} = -\frac{GMm}{r^3}\bar{r} \tag{3.2}$$

Dividing out the spacecraft mass we have Equation 3.3 which governs motion for the Restricted Two Body Problem. The restriction is due to the presupposed assumption that the Earth's mass M >> m which in the case of a spacecraft orbiting the Earth is definitely true. This assumption additionally fixes the coordinate system at the Earth's center since the spacecraft will have very little effect of the system's Center of Mass.

$$\ddot{\vec{r}} + \frac{GM}{r^3}\vec{r} = 0 \tag{3.3}$$

The zero to the right of the equal sign in Equation 3.3 results from our assumptions that there are only two bodies in the system providing accelerating forces. This equation, unfortunately, only approximately describes the motion of a spacecraft about the Earth. In reality there are small perturbations caused by other planets, atmospheric drag, the fact that the Earth is not really a point mass, etc. An expression of the form,

$$\ddot{\vec{r}} = -\frac{GM}{r^3}\vec{r} + \vec{a}_p \tag{3.4}$$

where a_p is the sum of all the perturbing accelerations, is more accurate. Whether to include certain accelerations in a_p depends on the order of magnitude of these perturbing forces acting on the body, and on the time interval over which they are allowed to affect its motion.

There are a plethora of possible solution methods used to solve the second order differential Equation 3.4 (Ref. 2). The distinguishing features between the different propagators is the manner in which this equation is solved. For the purposed of this thesis only three propagators are compared, they being the most popular.

A. THE COWELL PROPAGATOR

The Cowell propagator is the highest fidelity propagator used. It's accuracy is due to the fact that it solves the complete unsimplifed differential equation. It begins by breaking the second order differentials into two coupled first order different equations.

$$\begin{aligned} \dot{\vec{r}} &= \vec{v} \\ \dot{\vec{v}} &= -\frac{GM}{r^3}\vec{r} + \vec{a}_p \end{aligned} \tag{3.5}$$

These equations are solved simultaneously using a Runge-Kutta 4th order integrator. A built in feature of the code decreases the time step used in the numerical integrator scheme when the solution varies to rapidly over a short time interval. The step size is chosen in an effort to contain numerical truncation and rounding errors below a specified tolerance level.

While the Cowell propagator is generally the most accurate it is also the slowest. This is because it must perform the numerical computations over a relatively large number of small time steps in order to maintain accuracy. In addition, the time required significantly increases when atmospheric and/or gravity models are used to increase the propagator's accuracy.

B. THE CLOHESSY-WILTSHIRE PROPAGATOR

This propagator uses a set of linearized Equations of Motion for relative motion developed by Clohessy-Wiltshire. The derivation is taken from Reference 2 and Reference 3. The solution of the equations provides the position and velocity of a spacecraft, the chaser, with respects to another, the target. In order to define vectors between these two objects an orthogonol reference frame is attached to the target and moves with it. The coordinate system is a form of Local Vertical, Local Horizontal.

The vector position of the chaser is given by

$$\bar{r} = \bar{r}_T + \bar{\rho} \tag{3.6}$$

which is differentiated with respects to the M50 inertial coordinate system giving

$$\ddot{\bar{r}} = \ddot{\bar{r}}_T + \ddot{\bar{\rho}} + 2(\bar{\omega} \times \dot{\bar{\rho}}) + \dot{\bar{\omega}} \times \bar{\rho} + \bar{\omega} \times (\bar{\omega} \times \bar{\rho}) \tag{3.7}$$

where (omega) is the angular velocity of the target about the center of the Earth. If we take

$$\ddot{\bar{r}} = \bar{g} + \bar{a}_p \tag{3.8}$$

where g is the acceleration due to gravity and A is the acceleration due to external forces, Equations 3.7 and 3.8 can be resolved into x, y and z components.

$$
\begin{aligned}
\ddot{x} &= -g\frac{x}{r} + A_x + 2\omega\dot{z} + \dot{\omega}z + \omega^2 x \\
\ddot{y} &= -g\frac{y}{r} + A_y \\
\ddot{z} &= -g\left(\frac{z + r_T}{r}\right) + A_z + g_T - 2\omega\dot{x} - \dot{\omega}x + \omega^2 z
\end{aligned}
\tag{3.9}
$$

Assuming that the distance between the target and chaser is much smaller than the orbital radius of the target, i.e $(\rho)^2 << r^2_T$, the following approximations can be made

$$
\begin{aligned}
r &\approx r_T\left(1 + \frac{z}{r_T}\right) \\
g &\approx g_T\left(1 - \frac{2z}{r_T}\right) \\
-g\frac{x}{r} &\approx -g_T\frac{x}{r_T} \\
-g\frac{y}{r} &\approx -g_T\frac{y}{r_T} \\
-g\left(\frac{z + r_T}{r}\right) &\approx -g_T\left(1 - \frac{2z}{r_T}\right)
\end{aligned}
\tag{3.10}
$$

which by substitution into Equation 3.9 yields

$$
\begin{aligned}
\ddot{x} &= -g\frac{x}{r_T} + A_x + 2\omega\dot{z} + \omega z + \omega^2 x \\
\ddot{y} &= -g_T\frac{y}{r_T} + A_y \\
\ddot{z} &= 2\,g_T\frac{z}{r_T} + A_z + 2\omega\dot{x} + \dot{\omega}x + \omega^2 z
\end{aligned}
\tag{3.11}
$$

If we make the additional assumption that the target's orbit is circular, then

$$\dot{\omega} = 0$$

$$\omega = \sqrt{\frac{g_T}{r_T}}$$

and Equation 3.11 becomes

$$\begin{aligned} \ddot{x} &= A_x + 2\omega\dot{z} \\ \ddot{y} &= A_y - \omega^2 y \\ \ddot{z} &= A_z - 2\omega\dot{x} + 3\omega^2 z \end{aligned} \tag{3.12}$$

Since **y** is uncoupled from **x** and **z** in Equation 3.12, it can be solved simply and separately. Assuming a solution of the form

$$y = A\sin\omega t + B\cos\omega t + \frac{A_y}{\omega^2} \tag{3.13}$$

A and B are determined from the initial conditions, giving the solution

$$\begin{aligned} y &= y_o\cos\omega t + \frac{\dot{y}_o}{\omega}\omega sin\omega t + \frac{A_y}{\omega^2}(1 - \cos\omega t) \\ \dot{y} &= \dot{y}_o\cos\omega t - y_o(\omega\sin\omega t) + \frac{A_y}{\omega}\sin\omega t \end{aligned} \tag{3.13}$$

The equations for **x** and **z** are more difficult because they are coupled. We begin integrating the equation for **x** once and substitute the result into the equation for **z**.

$$\ddot{z} + 2\omega(2\omega z + A_x t + c_1) - 3\omega^2 z - A_z = 0 \tag{3.15}$$

Assuming that the solution to Equation 3.15 is of the form

$$z = A\sin\omega t + B\cos\omega t - \frac{2\omega A_x t}{\omega^2} - \frac{2\omega c_1}{\omega^2} + \frac{A_z}{\omega^2} \tag{3.16}$$

it can be substituted into the equation for x dot resulting in:

$$\dot{x} = 2\omega A \sin \omega t + 2\omega B \cos \omega t - 3 A_x t - 3 c_1 + 2\frac{A_z}{\omega} \tag{3.17}$$

Integrating,

$$x = -2A\cos \omega t + 2B\sin \omega t - \frac{3}{2}A_x t^2 - 3c_1 t + 2\frac{A_z}{\omega}t + c_2 \tag{3.18}$$

and applying the initial conditions we obtain

$$\begin{aligned} A &= \frac{1}{\omega}\left(\dot{z}_o + \frac{2}{\omega}A_x\right) \\ B &= \frac{2}{\omega}\dot{x}_o - 3z_o - \frac{A_z}{\omega^2} \\ c_1 &= \dot{x}_o - 2\omega z_o \\ c_2 &= x_o + \frac{2}{\omega}\left(\dot{z}_o + \frac{2}{\omega}A_x\right) \end{aligned} \tag{3.19}$$

Substituting and reordering terms,

$$\begin{aligned} x &= x_o + z_o\left[6(\omega t - \sin \omega t)\right] + \dot{x}_o\left[\frac{4\sin \omega t}{\omega} - 3t\right] + \dot{z}_o\left[\frac{2}{\omega}(1-\cos \omega t)\right] + A_x\left[-\frac{3}{2}t^2 + \frac{4}{\omega^2}(1-\cos \omega t)\right] + A_z\left[\frac{2}{\omega}(\omega t - \sin \omega t)\right. \\ y &= y_o[\cos \omega t] + \dot{y}_o\left[\frac{\sin \omega t}{\omega}\right] + \frac{A_y}{\omega^2}(1-\cos \omega t) \\ z &= \dot{x}_o\left[-\frac{2}{\omega}(1-\cos \omega t)\right] + z_o[4-3\cos \omega t] + \dot{z}_o\left[\frac{\sin \omega t}{\omega}\right] + A_x\left[-\frac{2}{\omega^2}(\omega t - \sin \omega t)\right] + A_z\left[\frac{1}{\omega^2}(1-\cos \omega t)\right] \\ \dot{x} &= \dot{x}_o[4\cos \omega t - 3] + z_o\left[6\omega(1-\cos \omega t)\right] + \dot{z}_o[2\sin \omega t] + A_x\left[\frac{4}{\omega}\sin \omega t - 3t\right] + A_z\left[\frac{2}{\omega}(1-\cos \omega t)\right] \\ \dot{y} &= \dot{y}_o \cos \omega t - y_o(\omega \sin \omega t) + \frac{A_y}{\omega}\sin \omega t \\ \dot{z} &= \dot{x}_o[-2\sin \omega t] + z_o[3\omega \sin \omega t] + \dot{z}_o[\cos \omega t] + A_y\left[-\frac{2}{\omega}(1-\cos \omega t)\right] + A_z\left[\frac{\sin \omega t}{\omega}\right] \end{aligned} \tag{3.20}$$

The Clohessy-Wiltshire equations are convenient since they give answers in LVLH coordinates. This implies, assuming the radius and velocity vectors are obtained by the chasing vehicle, that no coordinate transformation is required for orbit determination. A drawback the to the solution given above is that they are based upon the assumption that the target orbit is circular. This produces an inherent error in the algorithm whose magnitude varies with distance between the vehicles and eccentricity of the two orbits. The greater the distance and eccentricity the greater the magnitude. These disadvantages most likely make the Clohessy-Wiltshire Propagator the least accurate of the propagators used.

C. THE ENCKE PROPAGATOR

While the Cowell method is probably the most accurate propagation method it can be cumbersome and time consuming, especially if the perturbing acceleration is much smaller than the force of gravity. Because this is the case for an Earth orbiting spacecraft an alternative technique based upon integrating the vector difference between the Two Body Solution and the perturbed solution rather than the explicit state vector found in the Cowell Method. This is the idea behind the Encke Method. The particular version of the Encke method developed here is taken from Reference 4.

The Encke Method assumes that the spacecraft is traveling in a conical path called osculating orbit. This osculating orbit is determined by the position and velocity vectors at a given time t_o using the classical Two Body Problem. Because of the perturbing accelerations, the actual orbit diverges in time from the osculating orbit and these deviations are what is found by the method. These vector differences are then added to the osculating orbit position and velocity vectors to give the actual state vectors at a future time.

As stated previously, the osculating orbit is derived using the restricted two body. The method employed in Reference 4 is based upon the so-called "f" and "g" functions. These are determined from the position and velocity vectors at a prescribed time t_o, and can be used to generate the classical orbital element. The f and g functions are given in Equation 3 (Ref. 4).

$$
\begin{aligned}
f &= \frac{a}{r_o}\left[(\cos(E - E_o) - 1\right] + 1 \\
g &= \sqrt{\frac{a^3}{\mu}}\left[\sin(E - E_o) - (E - E_o)\right] + (t - t_o) \\
\dot{f} &= -\frac{\sqrt{\mu a}}{r_o r}\sin(E - E_o) \\
\dot{g} &= 1 - \frac{a}{r}\left[1 - \cos(E - E_o)\right]
\end{aligned}
\tag{3.21}
$$

Position and velocity vectors of the osculating orbit are given by:

$$
\begin{aligned}
\vec{r}_{osc} &= f\vec{r}_o + g\vec{v}_o \\
\vec{v}_{osc} &= \dot{f}\vec{r}_o + \dot{g}\vec{v}_o
\end{aligned}
\tag{3.22}
$$

In the Encke formalism, these vectors are used in the differential equation for the difference vector (δ):

$$
\frac{d^2\vec{\delta}}{dt^2} + \frac{\mu}{r_{osc}^3}\vec{\delta} = \frac{\mu}{r_{osc}^3}\left(1 - \frac{r_{osc}^3}{r^3}\right)\vec{r} + a_p \tag{3.23}
$$

To avoid difficulties in evaluating **r**, slight modifications to Equation 3.23 are made. Since

$$
\vec{r}(t) = \vec{r}_{osc}(t) + \delta(t) \tag{3.24}
$$

we have

$$
1 - \frac{r_{osc}^3}{r^3} = -F(q) = 1 - (1 + q)^{\frac{3}{2}} \tag{3.25}
$$

where

$$
q = \frac{\vec{\delta} \bullet \left(\vec{\delta} - 2\vec{r}\right)}{\vec{r} \bullet \vec{r}} \tag{3.26}
$$

The function F(q) can then substituted into Equation 3.23. This revised second order differential equation can now be integrated to find δ and its first derivative ν. When these are substituted into Equation 3.27, the position and velocity vectors for the desired time are found:

$$\begin{aligned}\vec{r} &= \vec{r}_{osc} + \vec{\delta} \\ \vec{v} &= \vec{v}_{osc} + \vec{\nu}\end{aligned} \qquad (3.27)$$

While this propagator is more accurate than the Clohessy-Wiltshire Propagator since it does not depend upon to circular orbits it does restrict itself, due to the method of determining the osculating orbit, to planar orbits. This means that greater error is likely in the out of plane direction, the y axis in the LVLH reference frame. Whether this error is significant is yet to be determined.

IV. THE PERTURBING ACCELERATIONS

The perturbing accelerations which affect the motion of a spacecraft in Earth's orbit are many. They are caused by physical phenomenon existing outside the orbital system, such as solar radiation, because as well as due to the fact that many of the assumptions made in developing the Restricted Two Body Problem are too simplistic. The simplifying assumptions inherent in the Two Body Problem, such as disregarding the existence of three body effects, cause errors in the predictions. Regardless of the source, these perturbing accelerations should be considered in the propagation techniques in order to insure accurate predictions.

A. THE PERTURBATIONS

When considering a Low Earth Orbit (LEO), just about every conceivable perturbing force has an effect. Each of them must be reviewed and either incorporated into the propagator or discarded depending upon the magnitude of the perturbation they produce.

1. Solar Pressure.

The perturbation known as solar pressure is caused by the impingement of solar photons on the surface of a spacecraft. One's first impulse is to discard this as negligible. Before doing so, one should consider that in space there is no counter force, such as atmospheric drag, to resist such a force. Over a sufficiently long time interval this perturbing force could build up to a significant level. Near Earth, the Solar Pressure Constant is 4.7×10^{-5} dynes/cm^2.

Typically Solar pressure effects the satellite's orbital eccentricity, but as implied above, it typically takes time for it's effects to be felt. The time frame over which the propagator must be accurate for the purpose of this research is one orbit, or approximately 90 minutes, and therefore this effect can be reasonably neglected.

2. Magnetic

The Earth's magnetic field, like any magnetic field, can induce a force on a magnetized or a current carrying body. The magnitude of this force is dependent upon the size of the magnetic fields and/or current. Such a force is often used by spacecraft via magnetic torquers to actively introduce a change in the spacecraft attitude. Even if there were no active use of the magnetic field, a spacecraft, after a sufficient time, develops a slight magnetic field.

The difficulties in using the Earth's magnetic field for atitude control is really a boon for an orbital propagator because the constantly changing direction and magnitude which creates great difficulties in developing a lengthy, direction-stable force does not create a very coherent perturbing force. Additionally, because the Earth's magnetic field is so weak, only a fairly large current in the orbiter creates an appreciable effect. For these reasons, magnetic perturbations are ignored in this thesis.

3. Third Body Effects

The reality of orbital mechanics is that there are several gravitating bodies rather that the two assumed in the Restricted Two Body Problem. The Moon, the Sun and the other planets all have a gravitational effect on an orbiting spacecraft. To accurately model these effects the system should be expanded from two bodies to three, four, etc. This was attempted for a three body system and was found to be analytically intractable except in very limited circumstances. Extensions to a system of four or greater bodies turns out to be of very limited value for practical matters involving orbiting satellites.

One possibility is to treat these effects like any other perturbation. It has been found that the accumulated effects, while they do exist, are again insignificant over the short duration of a single orbit. Therefore these perturbations are also ignored.

4. Earth Gravity Harmonics

The Restricted Two Body Problem assumes that the Earth is spherically symmetrical and therefore can be represented by a point mass. In reality it is a large semi-homogenous ball. For a point mass, it can be assumed that the force of gravity is constant at every point on a sphere encompassing that point mass. For a semi-homogenous ball, every point on that same sphere can experience a different gravitational force. In order to take this variation into account a model of this variation has been developed. In the case of gravity, the concept of a gravitational potential provides this model.

By mapping the gravitational potential at all points around the Earth it is possible to determine the acceleration due to gravity at any such point. The acceleration in a given direction is simply the gradient of the potential in that particular direction. The external geopotential is based upon

$$V = -\frac{\mu}{r}\left[1 + \sum_{n=2}^{N}\sum_{m=0}^{n}\left(\frac{a}{r}\right)^{n} P_n^m(\sin\phi)\left(C_{nm}\cos m\lambda + S_{nm}\sin m\lambda\right)\right] \tag{4.1}$$

where:

μ = The Earth's Gravitational constant

r = The magnitude of the spacecraft radius vector

a = The Semi-major axis of the Central ellipsoid (Earth)

n,m = Degree and order of each term

ϕ = Geocentric latitude

λ = Geocentric longitude

C_{nm}, S_{nm} = Gravitational coefficients

P_n^m = Associated Legendre functions

N = number of terms used

The Gravitational Coefficients can be broken into two categories, C_{n0} , the zonal harmonics or the C_{nm} , the tesseral and sectorial harmonics. The zonal harmonics are also know as the J_n coefficients of which J_2 is the most dominant. The harmonics define the shape and distribution of the Earth mass.

The J_2 effect can have a significant effect on a spacecraft's orbit in a short amount of time. For this reason a gravity model must be examined to see if it has any substantial effect. Also it must be determined to what fidelity, i.e. number of coefficients, the model should have.

5. Atmospheric Drag

The final perturbing force considered, is that due to atmospheric drag. Even as high as 1000 km the Earth has a measurable atmosphere. While it is true that it is essentially only an indistinct plasma, there are still particles which can impact a spacecraft and cause a change in velocity. Also, as the altitude decreases the atmosphere becomes more dense and therefore more of a factor.

For LEO spacecraft, atmospheric drag can be the dominant perturbing force. The drag a spacecraft feels is a function of velocity, atmospheric density and the spacecraft's ballistic coefficient. The velocity is constant for a circular orbit, but as discussed previously, orbits are never truly circular. For elliptical orbits velocity is constantly changing depending on the point along the ellipse. The fact that the atmosphere's density is also variable as a function of both position and time further complicates the problem. The ballistic coefficient can be assumed constant since it depends upon the shape of the Orbiter which does not change.

The fact that velocity and density are variable means that drag is constantly changing, typically in a very short time. As a result of this rapid change, Atmospheric Drag has the potential to significantly effect an orbital prediction. Velocity is easily gained from an osculating orbit model, but density often requires a very complex model.

B. THE MODELS

For the purpose of this thesis only two perturbing forces are used, Earth Gravitational Harmonics and Atmospheric Drag. There are numerous models, each with their own advantages and disadvantages. Models for this thesis were primarily chosen because of their availability, but fortunately, both are also extremely accurate.

1. The GEM-9 Geopotential Model

All Geopotential Models are essentially the same. Equation 4.1 is used to generate the gravitational potential at a specific location. They differ in the values of the gravitational coefficients and the number used. For this thesis the GEM-9 model using coefficients from Table 3 of Reference 5 are used. The model has a maximum resolution of 30 x 30, and uses the WGS-84 coordinate system. This is an ECEF standard coordinate system.

2. The Jacchia 71 Atmospheric Model

There are a number of potential Atmospheric models. Some are purely exponential, while others are more complex, taking into account the date, time, latitude and longitude and the effect of the sun on the upper atmosphere. The Jacchia Models are of the latter category making them large but more accurate. This model was developed by Jacchia in 1970 and takes into account the 11-year and 27-year solar cycles. It has the added advantage of using the WGS-84 coordinate system.

V. COMPARING PROPAGATORS

A. THE DATA SET

The easiest way to judge the accuracy of any algorithm is to compare it to actual data from the phenomenon being modeled. If the algorithm results in a relatively good match with the data the model and algorithm are considered acceptable. The usual tack taken by a modeler, is to start with the simplest model available to describe a phenomenon, and include effects (or fine tune the model) until such a time as the model is acceptable. It may happen that further refinement is possible but perhaps unnecessary to produce a workable model and algorithm. If not, it is generally back to the drawing board for the individual who is developing the model and algorithm.

The data set in this thesis comes from a rendezvous mission performed by the Space Shuttle, and consists of a series of state vectors for the Space Shuttle and a rendezvous target. Each state vector is comprised of the spacecraft's orbital position and velocity as well as a time stamp when the measurement was made. The entire data set has 3238 state vectors taken at approximately 3.5 seconds intervals. The data set, as seen in Figure 5.1, contains a record of two orbits during which time the Orbiter performs a rendezvous with the target vehicle. Unfortunately, it was determined near the end of the project that the data could have been processed using a high-fidelity propagator to fill in the gaps. This fact limits the possible accuracy to that provide by the high-fidelity propagator. It also could produce a more accurate prediction to appear less accurate.

In Figure 5.1, the data is presented as x versus z, but since the x coordinate closure rate is constant, the figure also demonstrates orbital positions as a function of time. All state vectors are provided in M50 inertial coordinates. Additionally, because the data is of an actual rendezvous, there are numerous thruster firings performed by the Orbiter during the time interval covered by the data set. These firings produce anticipated errors in the propagators, but since they are essentially impulses they are also readily identifiable.

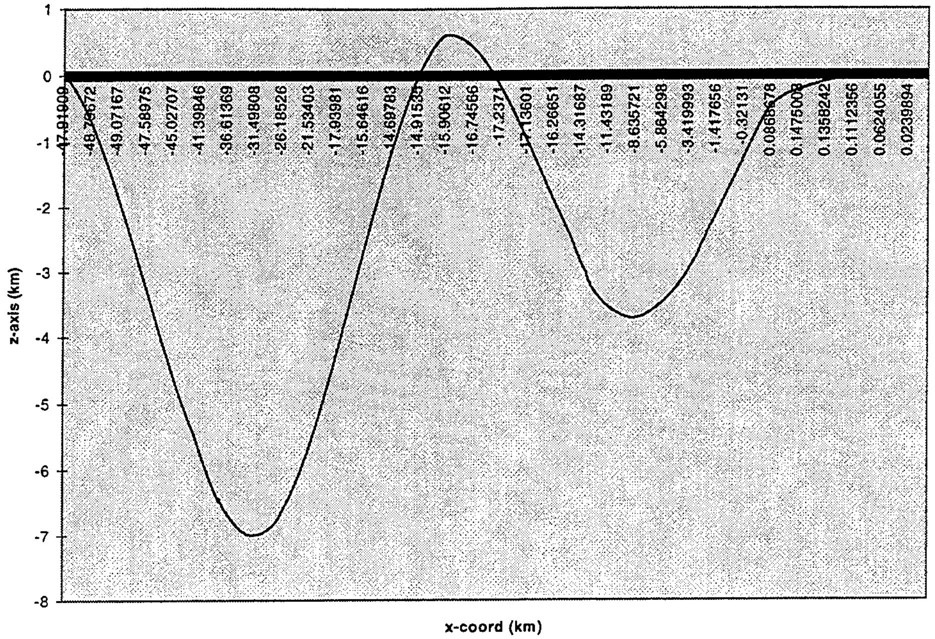

Figure 5.1 Data Set in LVLH Coordinates

B. THE PROGRAMS

Since the motivation for this thesis is the efficacy of various propagators in the development of the RPOP software, it seemed logical to retain the C++ coding of the actual candidates. The majority of the code used in this thesis is the NPSLite software developed by LT Lee Barker (Ref. 6), but numerous modifications and additional code has been written by the author.

The Cowell propagator used was originally developed by Robert Gottlieb and Mike Fraietta of McDonnell Douglas Corporation for NASA. Some code modification were made by LT Lee Barker (Ref. 6) to make the algorithm work. Additional modifications were incorporated by the author into the C++ code written for this thesis, but no changes to the core algorithm were made. In order to properly compare the performance of the Cowell propagator with the Clohessy-Wiltshire propagator, both the orbiter and the target state vectors were predicted and converted to the LVLH reference frame. This was to nullify any common errors made by the algorithms which might have occurred in both spacecraft predictions

The Clohessy-Wiltshire propagator was originally written by Scott Tamblyn of NASA's Johnson Space Center and Jack Brazzel of McDonnell Douglas. Modifications to this algorithm were made to incorporate perturbing accelerations. The perturbing accelerations include a Jacchia 70 atmospheric model and a GEM-9 gravity model coded for use by the Cowell propagator. By using the same perturbing accelerations as the Cowell, a potential source of error was eliminated. Both the orbiter state vector and the perturbing accelerations had to be converted from the inertial frame to the LVLH frame prior to use by the Clohessy-Wiltshire propagator.

The Encke Propagator used the "f and g" functions developed by LT Les Makepeace (Ref. 1) and coded by LT Barker (Ref. 6) for NPSLite. A Runge-Kutta 4-5 integrator which integrates Equation 3.23 was incorporated by the author. Gravitational and atmospheric models were once again taken from the Cowell propagator to maintain coherence in the project. As with the Cowell propagator, state vectors were predicted in inertial coordinates and then converted to LVLH for the purpose of comparison.

Numerous difficulties were experienced in compiling and running the Encke propagator when the gravitational and atmospheric models were added. Without the additional models the Encke propagator ran well. Addition of the perturbing forces caused a divergence of the orbit predictions. Unfortunately there was insufficient time to track this error down, and therefore an interesting portion of the project could not be accomplished.

C. PERFORMANCE

The performance of the different propagators has not been judged solely on the accuracy of the predicted state vectors, but also on how that accuracy varied as the time step is increased. Additionally, the amount of computation time required to perform the propagation is compared. It was anticipated that in order to obtain the most accurate prediction, a high fidelity propagator would be needed to break up the prediction time interval into a series of smaller time steps over which each propagator could be run. Ideally, the propagator requiring the shortest computation time over the largest acceptable time step would optimize performance.

For the purpose of this project four time steps were chosen. The smallest step was based on the separation between consecutive state vectors in the data set, approximately 3.84 seconds. In order to insure that actual state vectors would be available for comparison, the remaining three time steps were simply a factor two, five and ten times that base time step. This resulted in time steps of 7.68, 19.2 and 38.4 seconds. Average computation time was determined by dividing the total amount of time required to propagate all 3238 state vectors over all four time steps by the total number of state vectors propagated.

D. FINDINGS

The Cowell and Encke propagators proved to be the most accurate as seen by Figure 5.2 (a) and (b). The Encke Coordinate and Velocity Differentials were virtually identical to those of the Cowell method. Differentials is defined as the difference between the actual state vector and the predicted state vector.

The times represented on the x-axis of the two figures is in term of seconds since the beginning of the calendar year accordance with the time step of each state vector.

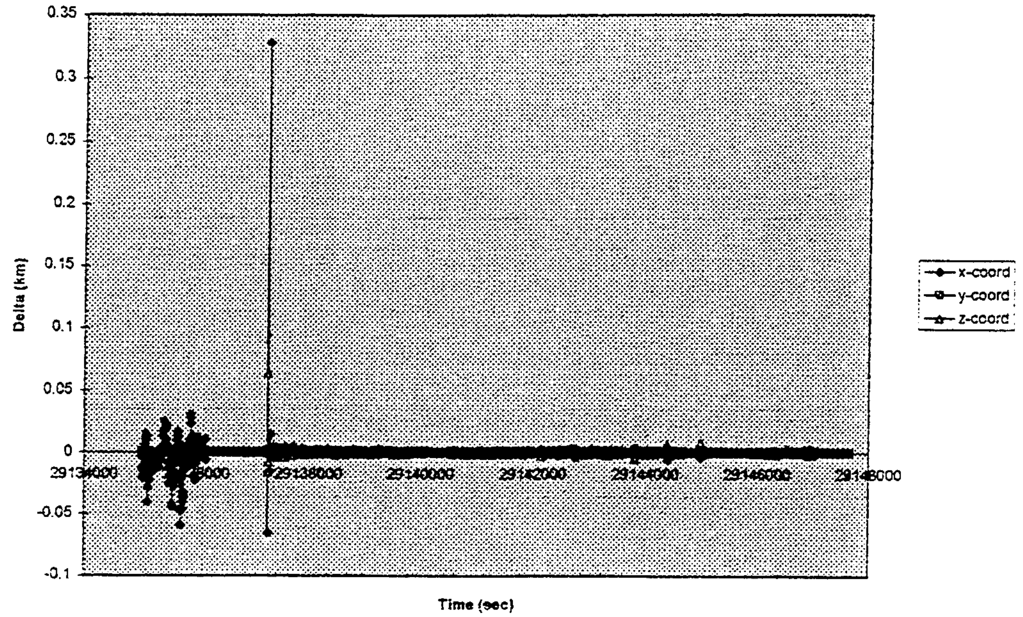

Figure 5.1 (a) Position Differential of Cowell Propagator for 3.84 Time Step

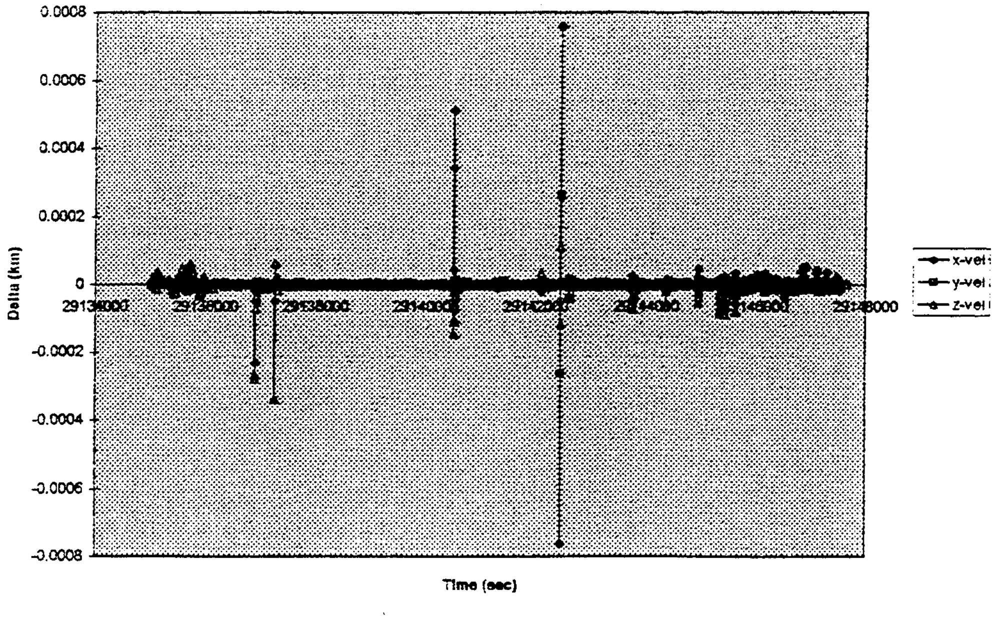

Figure 5.2 (b) Velocity Differential of Cowell Propagator for 3.84 Time Step

The Clohessy-Wiltshire propagator predicted sinusoidal variations as seen in Figures 5.3 (a) and (b). The cause of the sinusoidal motion is a result of the initial assumption in deriving the Clohessy-Wiltshire Equations that the target orbit is circular. In reality the target orbit is more nearly elliptical, thereby introducing an error. This fact was discussed in Chapter III, Section B.

Additionally, large errors caused by thruster firings can be seen in both Figures 5.3 and 5.4. The largest of these occur at identical times with the Encke, Cowell and Clohessy-Wiltshire propagators, but notice that the Clohessy-Wiltshire is more susceptible to small firings judging form the relatively large number of spikes occurring in Figure 5.3 compared to those in Figure 5.2.

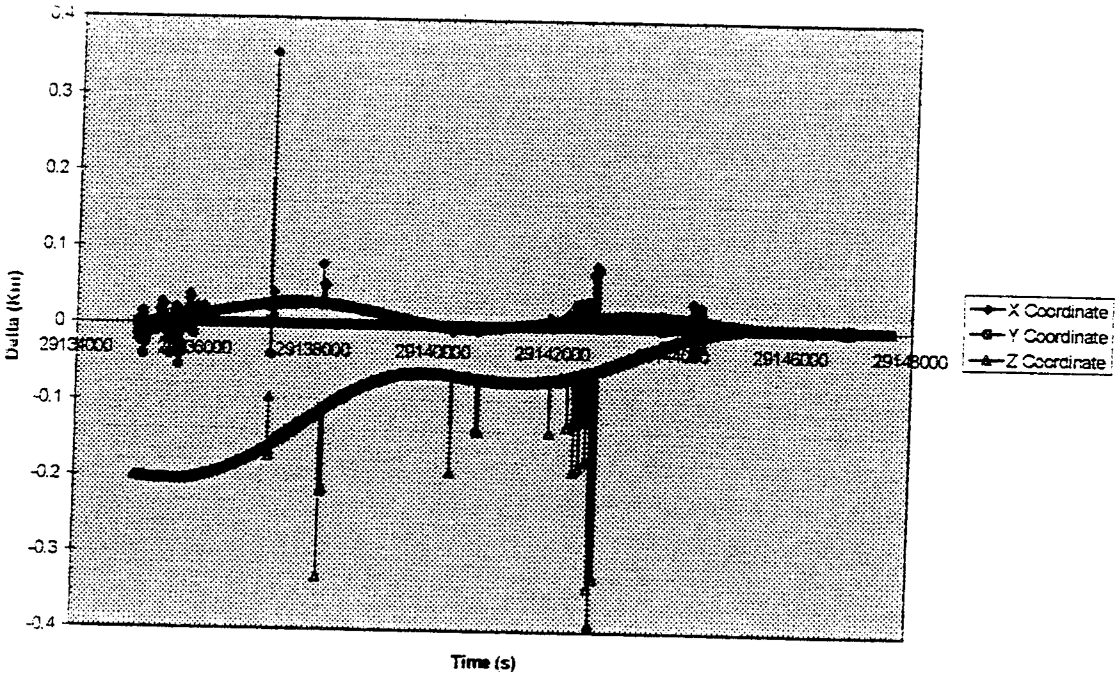

Figure 5.3 (a) Position Differential of CW Propagator for a 3.84 Time Step

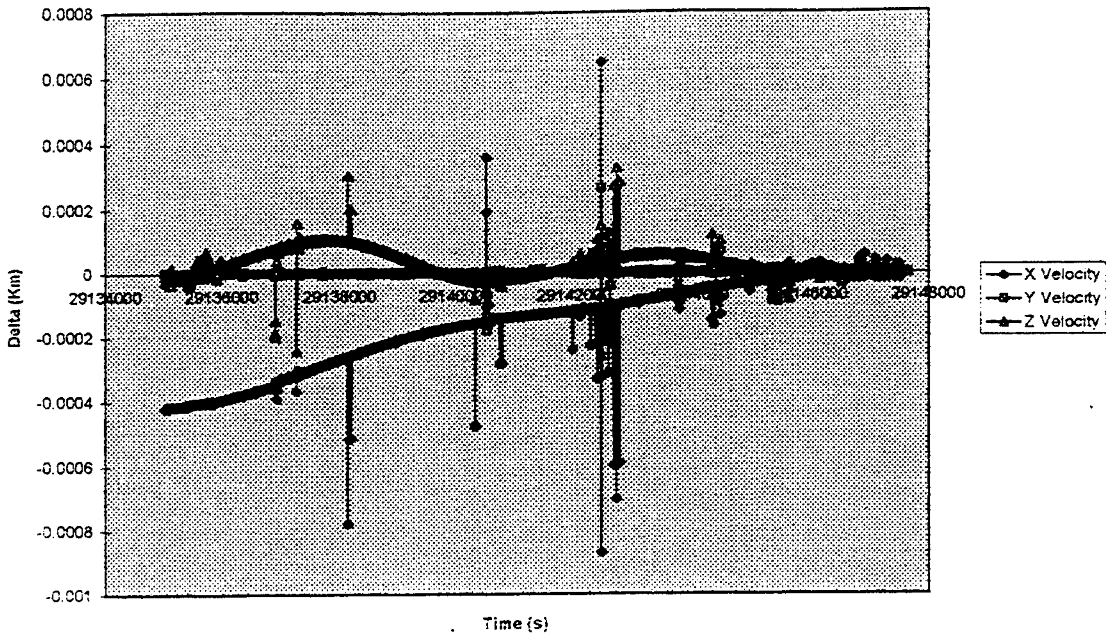

Figure 5.3 (b) Velocity Differential of CW Propagator for 3.84 Time Step

It is easier to view the separate differences in the three propagators when they are compared with respect to Position and Velocity Components. This type of comparison also makes it possible to see the differences produced by adding perturbing accelerations to the Clohessy-Wiltshire propagator. For the purpose of this analysis the gravity model is applied at two different resolutions to determine whether or not the number of tesserals and sectorials is significant. Also the atmospheric model and gravity models are applied both separately and together.

Additionally all propagators demonstrated a sinusoidal nature in the differentials. The commonality tends to suggest that it is the data set that is the cause vise the propagators. Possibly the error is a result of the manner in which the measurements were taken. An accelerometer, for example, can demonstrate a slight sinusoidal motion not caused by external accelerations.

Figure 5.4 displays the X Coordinate Differential. This graph denotes the difference between the predicted state vector and actual state vector for the same time verses increasing propagation time steps. Each differential is the average result of propagating all 3238 state vectors the appropriate time step and taking the difference. As expected, the Cowell propagator shows the smallest differential even at the largest time step. The Encke propagator parallels the Cowell's performance with error most likely due to its assumption of perfect elliptical motion. The Clohessy-Wiltshire shows the worst performance. The atmospheric model produced no apparent effect which really is not that surprising considering the low density of the atmosphere coupled with the short time steps consider. The fact that the addition of the gravitational model resulted in a worse solution not a better lends credence to the possibility that the data set contains processed state vectors not raw state vectors.

In Figure 5.5 the Y Coordinate Differential is shown. All propagators show almost identical error, including the end point of the unperturbed Clohessy-Wiltshire. This may appear unusual until the magnitude of the Delta's is examined, which at their worst never exceed 0.3 meters. The small magnitude of this error is because the motion of both the Orbiter and Target spacecraft are in very nearly the same orbital plane. Considering the small value of the input component the error is proportionately small.

The Z Coordinate Differential, shown in Figure 5.6, shows predictable results. Again the Cowell and Encke propagators are essentially error free. The addition of gravitational and atmospheric drag perturbations in the Clohessy-Wiltshire produce a negligible effect. The reason for the negligible difference when the perturbing forces are added is most likely due to the magnitude of the velocity in the z-direction. Since atmospheric drag in a specific direction is a function of the velocity of the spacecraft in that direction, and because the x-axis of the coordinate system used is defined by the spacecraft's velocity vector, drag can be expected to have a greater effect in the x-direction than in the z.

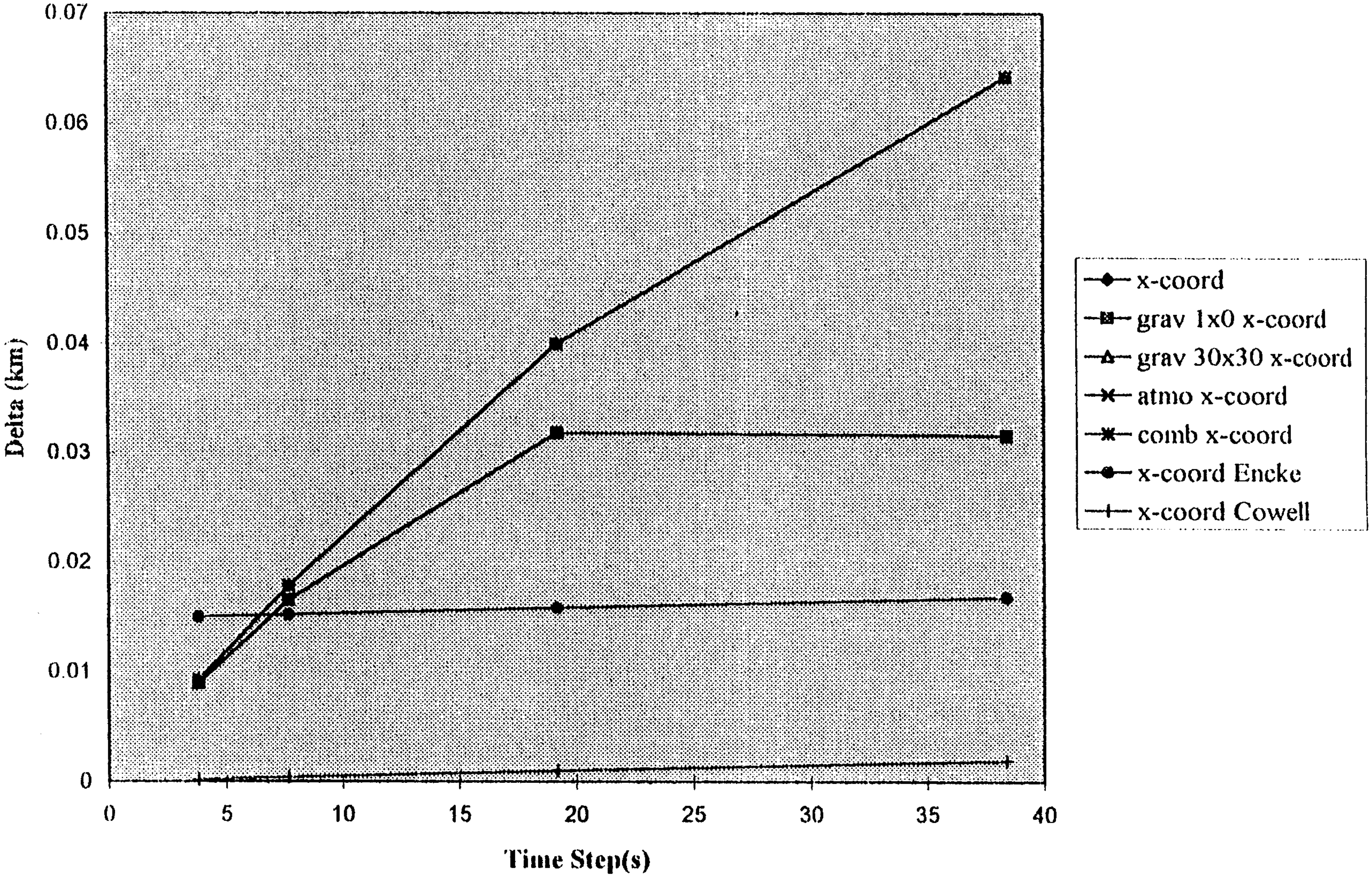

Figure 5.4 X Coordinate Differential

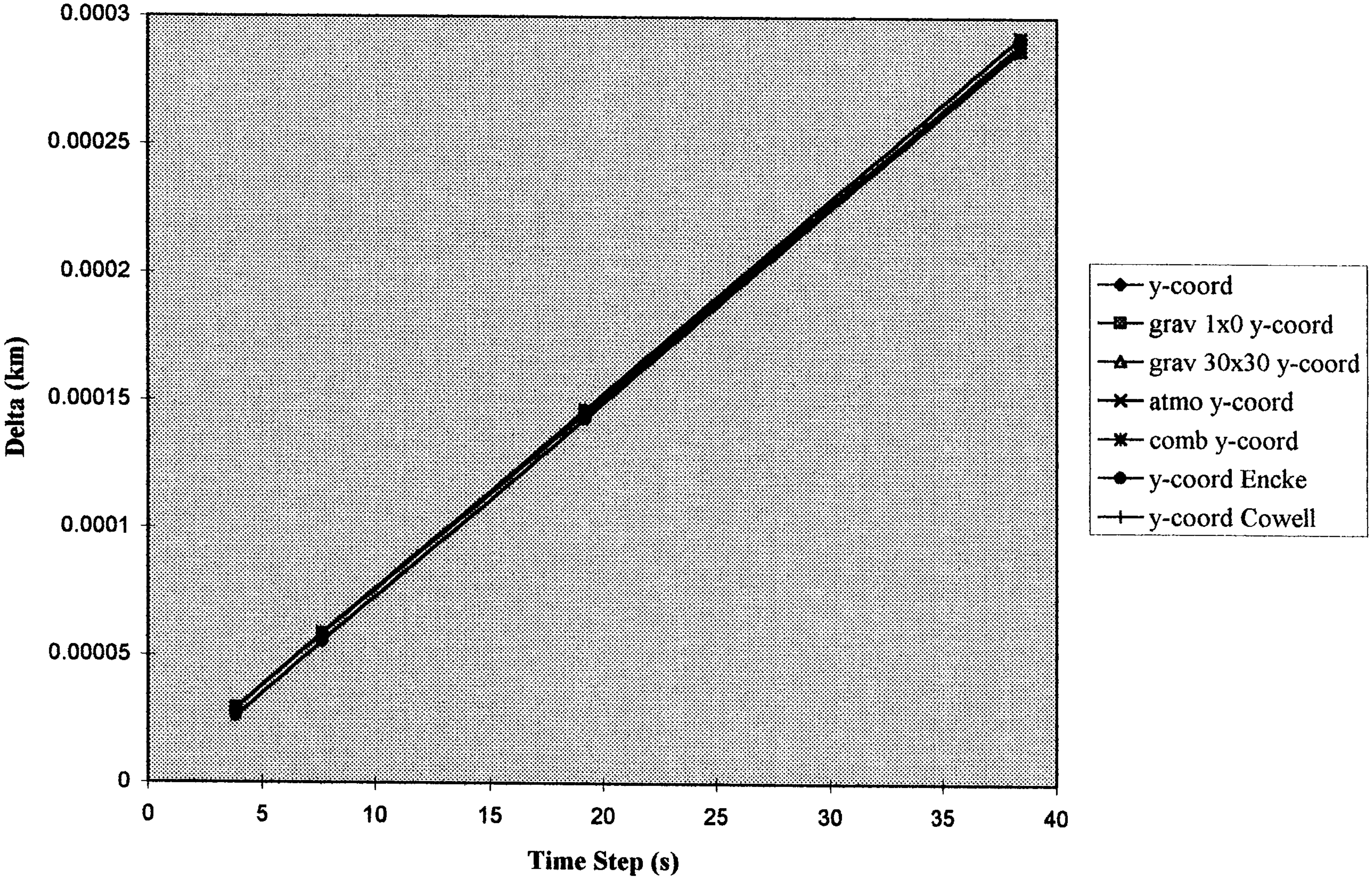

Figure 5.5 Y Coordinate Differential

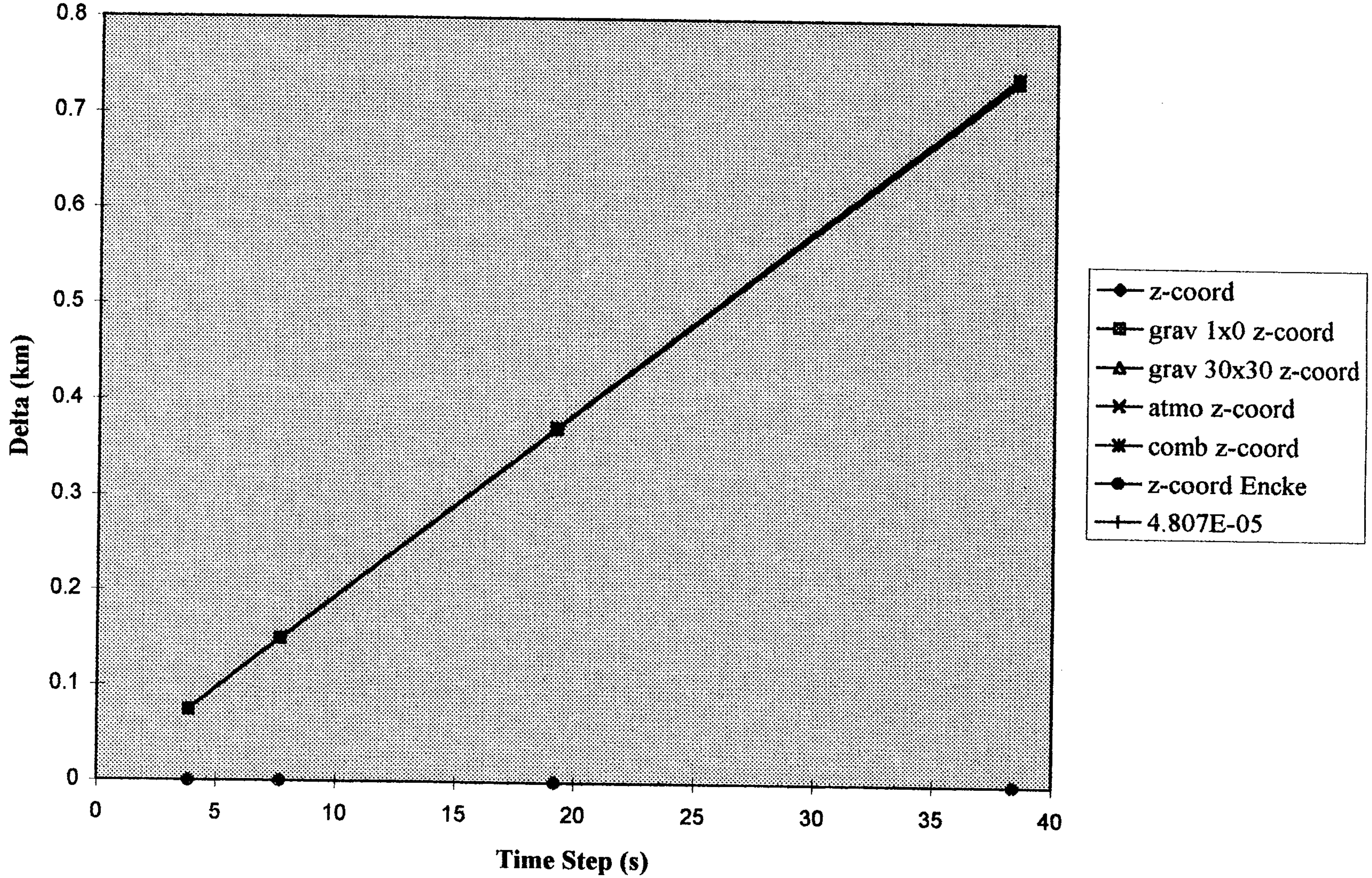

Figure 5.6 Z Coordinate Differential

Over the given time interval, the velocity components never exceed 7.5 km/s while the velocity differentials are all less than 2.5 m/s. Figures 5.7, 5.8 and 5.9 show the Velocity Differentials produced. In all three cases the Cowell propagator displays the least error. The Encke propagator is generally the second most accurate, except in the case of the Y Component where the Encke incurs it's greatest relative error. The source of this error can be traced back to the initial assumption made in deriving the "f and g" functions, which is that all motion is assumed to occur in the orbital plane, also known as the x and z plane. Therefore the variation in the component is a measure of the changes in out of plane relative velocity of the Orbiter and Target occurring over the time interval. This effect probably would be seen in the Y Position Component if the time interval had been greater.

E. COMPUTATION TIME

The computation times required for the each propagator can be seen in Table 5.1. They were determined by reading the computer's biostimer at program start and finish and dividing the difference by the number of vectors propagated. As expected, the Clohessy-Wiltshire proved the quickest with Encke next and the Cowell taking the longest time. Adding the perturbation models significantly increase the computation time of the Clohessy-Wiltshire, with little, if any, increase in accuracy. In fact, Encke propagator without any perturbations proved to be more accurate with the second shortest computation time.

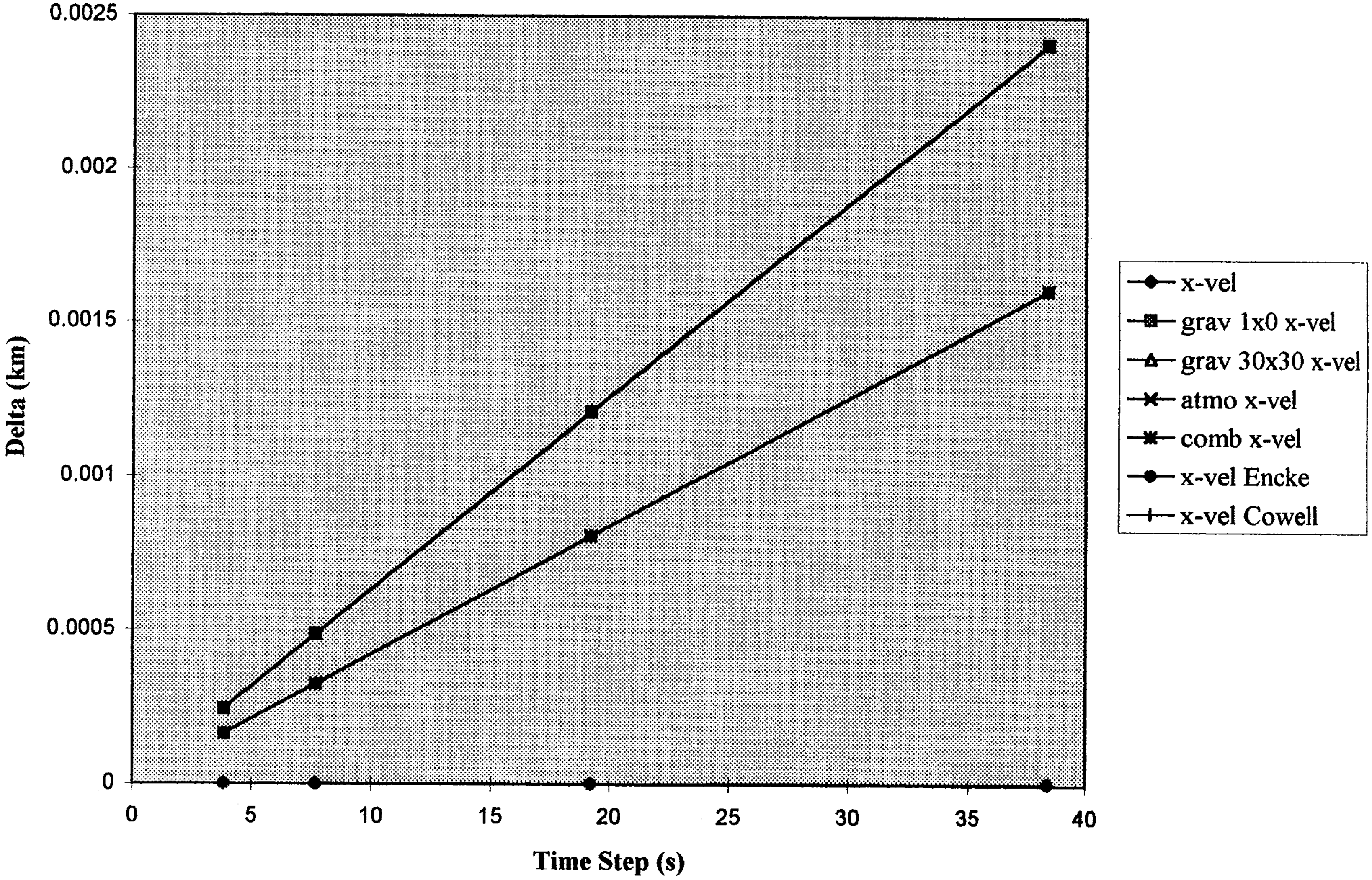

Figure 5.7 X Velocity Differential

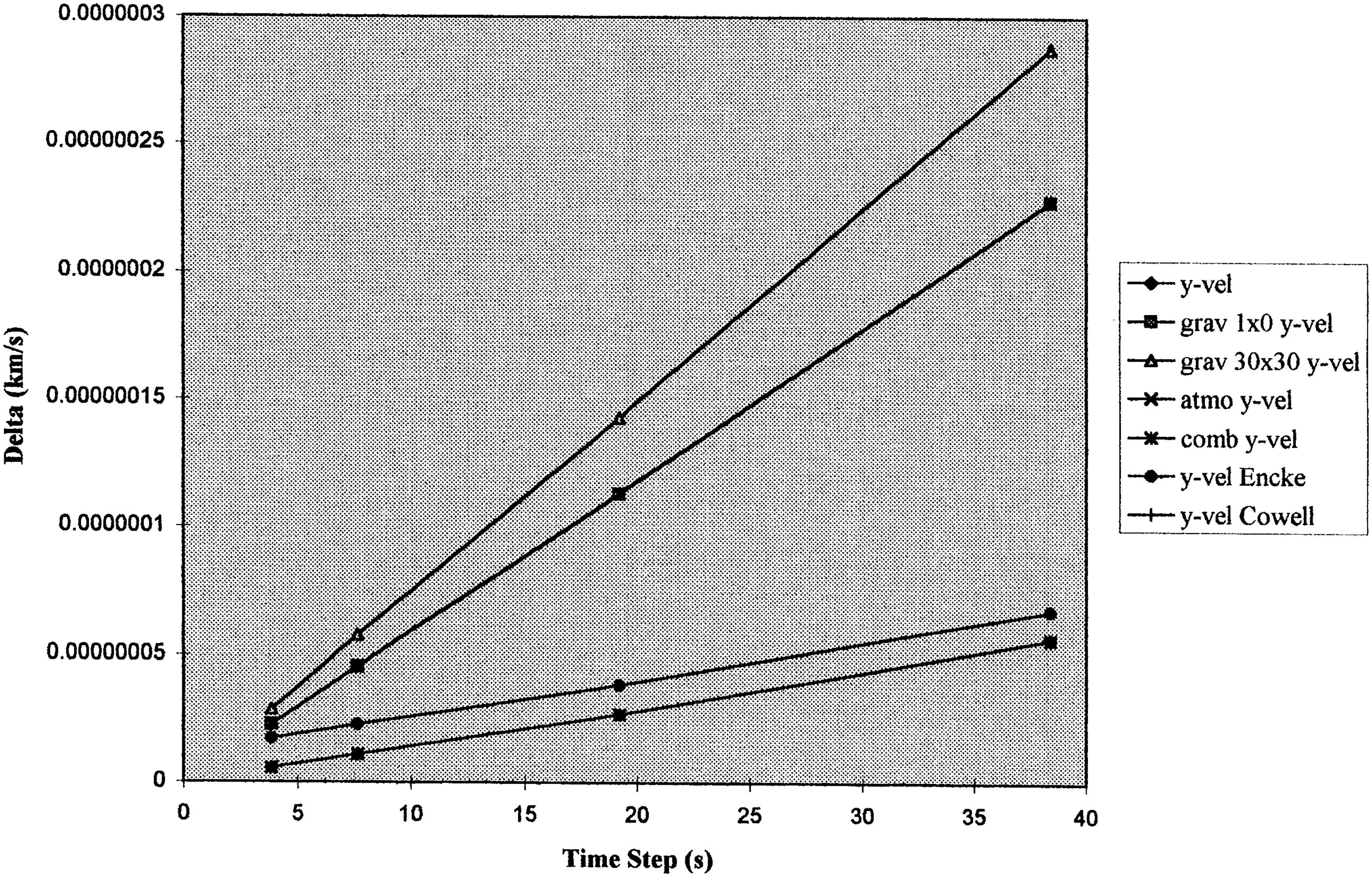

Figure 5.8 Y Velocity Differential

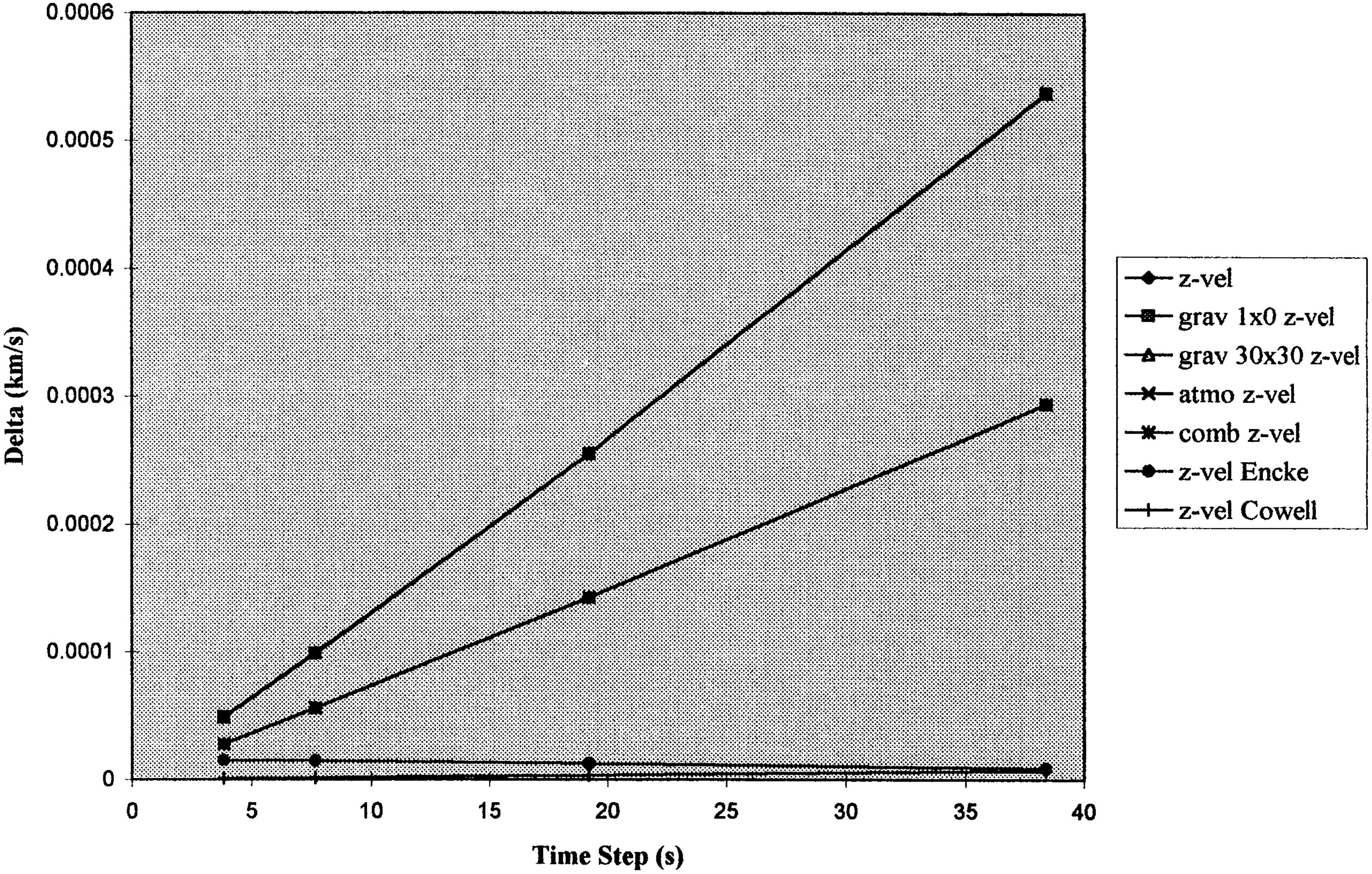

Figure 5.9 Z Velocity Differential

seconds/vector	Cowell	Encke	Clohessy-Wiltshire
Unperturbed	n/a	0.0167	0.0140
Gravitational 1x0	n/a	n/a	0.0501
Gravitational 30x30	n/a	n/a	0.0796
Atmospheric	n/a	n/a	0.0413
Atmospheric & Gravitational 1x0	0.1303	n/a	0.0589

Table 5.1 Propagator Computation Times

VI. CONCLUSIONS

The analysis performed by this thesis has attempted to determine which of three representative orbital propagators demonstrates the best performance. This performance determination is based not only on the accuracy of the propagator, but also on the computation time the propagator requires. Coupled with both of these criteria is the question of whether a propagator should apply the extensive models required for perturbing accelerations. Is the gain in accuracy worth the increased time required to compute the results.

A. THE RESULTS

As expected the Cowell propagator demonstrated the most accurate result while the Clohessy-Wiltshire required the least computational effort. As feared the perturbing accelerations produced a less accurate solution. This should be impossible, therefore the data set used must have been of processed data. This fact does not completely discount the project findings because a relative performance between the propagators can be inferred based upon the unperturbed results.

The greatest performance appears to be demonstrated by the Encke propagator which without the addition of perturbing accelerations is essentially the "f and g" functions. The Encke propagator demonstrated near Cowell accuracy with near Clohessy-Wiltshire computation times. Only in propagation of the **y** velocity component did the Clohessy-Wiltshire demonstrate superior performance to that of the Encke methodology.

B. ADDITIONAL WORK

In order to fully complete this project a number of things need to be accomplished.

1. Raw Data

The entire thesis should be repeated using the raw state vectors from a single sensing source. This sensing source need not be specified, but the data set used must not have been previously subjected to a propagator in order to smooth the data set as was probably done in this case. The C++ code developed in this thesis is already set up to perform this analysis whenever an appropriate data set can be found.

2. Encke Propagator

While the Encke Propagator worked extremely well without perturbing accelerations, this project still requires a working Encke propagator with perturbing accelerations in order to determine the potential benefits of adding these. The core work and theory exists, but the difficulties in compiling and executing the C++ code must be resolved. It is not anticipated that the addition of perturbing accelerations will result in any significant improvement in the algorithms performance for the short time interval calculations. This is especially true if one considers the fact that addition of the perturbing accelerations significantly increases computation time.

3. Repeated Iterations

The propagators should also be modified to check for the accuracy of the algorithms over longer propagation time in order to define the propagator limits. This could probably be done by breaking the propagation time into a series of sufficiently small time steps to maximize performance. This is identical to the method used in the Cowell propagator. In this method the state vector would be propagated over a series of time steps with the resulting state vector being used in successive iterations. The stability of the algorithms as well as the additive effects of error should be critically examined. Should an operational algorithm be developed using one of the propagators reviewed in this thesis, such an analysis should be done in the selection process.

4. Different Orbits

This and the above projects should also be repeated for different orbits to determine which performs best under those circumstances. More detailed knowledge is needed of the limits at which the perturbing forces are required. In this thesis, some of the possible perturbations were discarded purely based on logical assumptions. These could be examined. Additionally the perturbations used probably have limits which should be examined.

LIST OF REFERENCES

1. Makepeace, L. B., *Theoretical Basis for State Vector Comparison, Relative Position Display, and Relative Position/Rendezvous Prediction*, Naval Postgraduate School, Monterey, California, December 1993.
2. Chobotov, V. A., *Orbital Mechanics*, American Institute of Aeronautics and Astronautics, 1991.
3. Jackson, W. L., *Relative Motion EOM for Contstant Accelerations*, U.S. Memorandum EH2-86M-104, Lyndon B. Johnson Space Center NASA, 10 February 1986.
4. Battin, R. H., *An Introduction to the Mathematics and Methods of Astrodynamics*, American Institute of Aeronautics and Astronautics, 1987.
5. Lerch, F., *Gravity Model Improvements Using Geos 3 (GEM 9 and GEM 10*, Journal of Geophysical Research, Vol. 84, No. 88, 30 July 1979.
6. Barker, L. A., *NPS State Vector Analysis and Relative Motion Plotting Software for STS-51*, Navel Postgraduate School, Monterey, California, March 1994.

Initial Distribution List

1. Defense Technical Information Center 2
   Cameron Station
   Alexandria, Virginia 22304-6145

2. Library, Code 52 2
   Naval Postgraduate School
   Monterey, California 93943-5002

3. Clyde Scandrett (Code MA\Sd) 1
   Department of Mathematics
   Naval Postgraduate School
   Monterey, California 93943-5216

4. I. Michael Ross (Code AA\Ro) 1
   Department of Aeronautics and Astronautics
   Naval Postgraduate School
   Monterey, California 93943-5000

5. Chairman, (Code AA) 1
   Department of Aeronautics and Astronautics
   Naval Postgraduate School
   Monterey, California 93943-5000

6. Chairman, (Code SP) 1
   Space Systems Academic Group
   Naval Postgraduate School
   Monterey, California 93943-5000

7. Donald Danielson (Code MA/Dd) 1
   Department of Mathematics
   Naval Postgraduate School
   Monterey, California 93943-5216

8. Terry Alfriend 1
   Space Systems Academic Group
   Naval Postgraduate School
   Monterey, California 93943-5000

9. Jack Brassel 1
   McDonnell Douglas Space Systems
   Houston Division
   13100 Space Center Blvd
   Houston, Texas 77059-3556

10. Scott Tamblyn 1
Code EG431
NASA, Johnson Space Center
Houston, Texas 77058

11. Brent Jett 1
Astronaut Office - CB
NASA, Johnson Space Center
Houston, Texas 77058